A True Digital Feedforward Active Noise Control System with no Analog-to-Digital and Digital-to-Analog Converters

Mingzhe Li*, Chuang Shi†, and Yue Wang‡
University of Electronic Science and Technology of China, Chengdu, China
* E-mail: lmzhe@std.uestc.edu.cn
† E-mail: shichuang@uestc.edu.cn
‡ E-mail: wangyue2020@std.uestc.edu.cn

***Abstract*—An active noise control (ANC) system emits sound waves to attenuate noise. With constraints on cost and size, the ANC system often outperforms passive noise control (PNC) measures when the noise frequency is low. Electro-acoustic devices, such as microphones and loudspeakers, are conventionally used in ANC systems. They convert sound pressure with different voltages. The analog-to-digital and digital-to-analog converters have to be connected to the digital controller in the ANC system with electro-acoustic devices. With the development of digital acoustic devices, sound pressure can be converted straightforwardly into and from the digital signal in the format of pulse density modulation (PDM), which is also known as the 1-bit quantized signal. Incorporating with the digital acoustic devices, this paper proposes a true digital ANC system design that has no analog-to-digital (AD) and digital-to-analog (DA) converters. Specifically, the feedforward filtered reference least mean square (LMS) algorithm with online secondary path modeling is implemented in a newly proposed systolic structure on the FPGA, where the digital acoustic devices are connected directly to the FPGA I/O pins.**

I. Introduction

With the rapid industrialization and development of cities, noise generated by the increasing usage of machinery has begun to negatively impact the quality of city-dweller's living environment. Noise control methods has therefore gained increasing importance and significance. PNC methods obstruct or absorb noise waves by using sound diffracting structures and absorbing materials. However, it has been proven to be less effective in eliminating low-frequency noise when there are limitations in cost and size.

ANC was introduced as a new technique in the first half of the 20th century. It emits an anti-noise sound wave to destructively interfere with the noise wave. ANC methods can reduce low-frequency noise levels more efficiently than PNC methods [1]. Since the 1980s, with the development of adaptive filtering theory and large-scale integrated circuits, ANC applications have become feasible. To date, ANC methods have been used a wide range of applications in noise engineering scenarios such as commercial, industrial and military settings [2], [3].

Feedforward ANC (FFANC) system is preferable when dealing with broadband noise [4]. In addition to an error microphone for detecting residual noise, FFANC system requires a reference microphone to be placed close to the noise source, such that noise information from the noise source is acquired in advance for the pre-emptive calculation of the anti-noise waveform. Therefore, a modern FFANC system typically consists of a digital controller, several electro-acoustic devices, AD and DA converters [5], [6]. The digital controller performs real-time adaptive processing. The electro-acoustic devices, such as microphones and loudspeakers, convert sound pressure into and from analog signals. AD and DA converters, connecting the digital controller with those electro-acoustic devices, are in charge of the conversion between digital signals and analog signals.

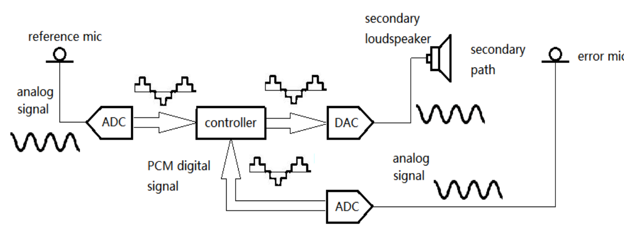

(a) Conventional FFANC System with AD and DA converters

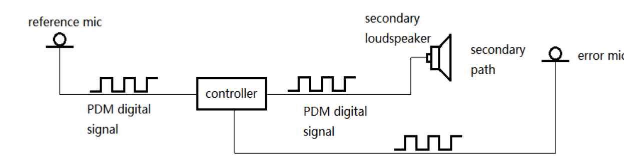

(b) True Digital FFANC System without AD and DA converters

Fig. 1: Comparison of FFANC system architectures.

Digital acoustic devices can transfer sound pressure into

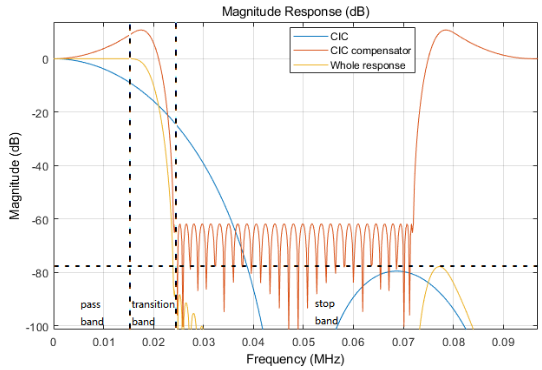

Fig. 2: Magnitude responses of the CIC filter and the CIC compensator in the PDM demodulator.

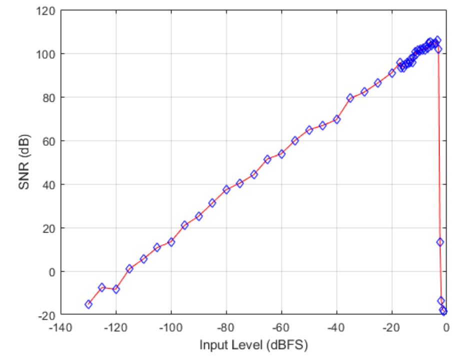

Fig. 3: SNR of the 4th-order PDM modulator.

and from digital signals directly in the PDM format [7]. The PDM is also known as the 1-bit quantized signal, where very high oversampling ratio (OSR) is adopted to reduce baseband quantization noise [8]. With digital acoustic devices, this paper proposes a true digital FFANC system without the use of AD and DA converters. PDM microphones convert sound pressure into PDM signals which can be processed by digital controller directly. Similarly, PDM loudspeakers convert PDM signals that are output from the digital controller into sound waves. As shown in Fig. 1, digital acoustic devices can be directly connected to the digital controller, streamlining and simplifying the architecture of the FFANC system. Last but not least, in the true digital FFANC system, the FPGA rather than the microprocessor is preferably chosen to implement the digital controller due to its high clock rate and flexible I/O pins [9], [10], [11].

II. System Design

There are three function modules in the digital controller of the true digital FFANC system. They are the PDM demodulator, the ANC algorithm with online secondary path modeling, and the PDM modulator.

A. PDM Demodulator

When demodulating PDM signals, the cascaded integrator-comb (CIC) filter is carried out [12], [13]. The system function of the CIC filter is written as

$$CIC(z) = (\frac{1}{N}\frac{1-z^{-N\times D}}{1-z^{-1}})^k \tag{1}$$

where N denotes the decimation factor in the CIC filter; k represents the number of integrators and the number of combs in cascade; and D is the differential delay of every comb. There is no multiplier in the CIC filter. When the decimation factor is exactly an integer power of 2, the divider after the integrators can also be implemented by a bit shifter. Therefore, the CIC filter is well known for its efficiency.

However, (1) shows that the frequency response of the CIC filter is a $sinc$ function, of which the transition band is unfavourably wide. Furthermore, when the CIC filter provides sufficient attenuation in the stopband, the passband is also attenuated notably. To solve this problem, a finite impulse response (FIR) filter is designed after the CIC filter to compensate the passband attenuation and improve the passband flatness. This FIR filter is also called the CIC compensator. Taking the PDM signal with a clock rate of 3.072 MHz as an example, the target audio bandwidth is from 0 to 15 kHz and the target sampling rate of the audio signal is 48 kHz. The OSR is 64. The CIC filter is designed with $N = 32$, $k = 6$, and $D = 2$. The CIC compensator considers the transition band from 15 kHz to 24 kHz and the stopband above 24 kHz. The magnitude responses of the CIC filter and the CIC compensator are shown in Fig. 2. The resultant whole response has the stopband attenuation of nearly 80 dB and the passband ripple less than 0.1 dB.

B. PDM Modulator

PDM signals are generated from the 1-bit quantization. The quantization noise is uniformly spreading over the entire bandwidth. The OSR has to be in a very high range, in order for the audio bandwidth to occupy a very small portion of the entire bandwidth. Both the audio signal and the quantization noise are shaped by digital filters, whose transfer functions are respectively denoted as $STF(z)$ and $NTF(z)$. The PDM signal is therefore written in the z domain as

$$V(z) = STF(z)A(z) + NTF(z)Q(z), \tag{2}$$

where $A(z)$ and $Q(z)$ denote the audio signal and the quantization noise in the z domain, respectively [14], [15].

Considering the same example as aforementioned, a 4th-order PDM modulator is designed as

$$NTF(z) = \frac{(z^2-2z+1)(z^2-1.998z+1)}{(z^2-1.492z+0.5643)(z^2-1.701z+0.7868)} \tag{3}$$

and

$$STF(z) = \frac{0.0061001z^2}{(z^2-1.492z+0.5643)(z^2-1.701z+0.7868)}. \tag{4}$$

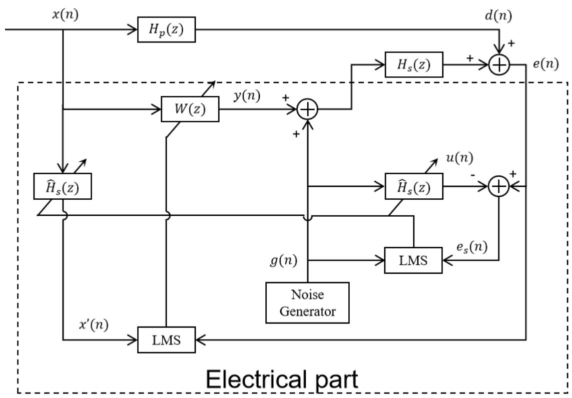

Fig. 4: Block diagram of the online modeling algorithm with additional white noise.

The signal-to-noise ratio (SNR) of the 4th-order PDM modulator is shown in Fig. 3, when the input signal is a sine wave at 12 kHz. As the input amplitude increases, the SNR of the modulator also improves. It achieves a peak value of 107.52 dB when the input amplitude reaches -3.5 dBFS.

C. ANC Algorithm with Online Secondary Path Modeling

In an ANC system, there is a complex path between the output of the ANC controller and the target zone of quiet, which is called the secondary path. ANC algorithms have been developed to cater for the secondary path. The filtered-reference least mean square (FxLMS) algorithm is the most commonly used [16], [17]. In the FxLMS algorithm, the secondary path is modeled by a digital filter, which is used to calculate the filtered reference signal based on the raw reference signal. The accuracy of the secondary path model can dramatically affect the performance of the FxLMS algorithm [18]. In order to model the secondary path continuously, Eriksson and Allie proposed an online modeling algorithm with additional white noise based on the FxLMS algorithm [19]. The block diagram of the online modeling algorithm with additional white noise is shown in Fig. 4, where $H_p(z)$ is the primary path; $W(z)$ is the control filter; $H_s(z)$ is the secondary path and $\hat{H}_s(z)$ is the secondary path model. The output of the control filter is superimposed with uncorrelated white noise that excites another LMS iteration to update the secondary path model.

Based on the systolic FxLMS structure [20], this paper proposes the systolic structure of the online modeling algorithm with additional white noise for its implementation on the FPGA. Two basic units are designed and implemented first. They are the filter unit (FU) and the LMS unit (LU), as shown in Figs. 5(a) and (b). The FU consists of an adder, a multiplier, a delay unit and a multiplexer, while the LU consists of an adder, a multiplier, a delay unit and 2 multiplexers. The LUs and FUs are interconnected as shown in Fig. 5(c) to carry out a complete online modeling algorithm with additional white noise that involves three filters and two LMS iterations.

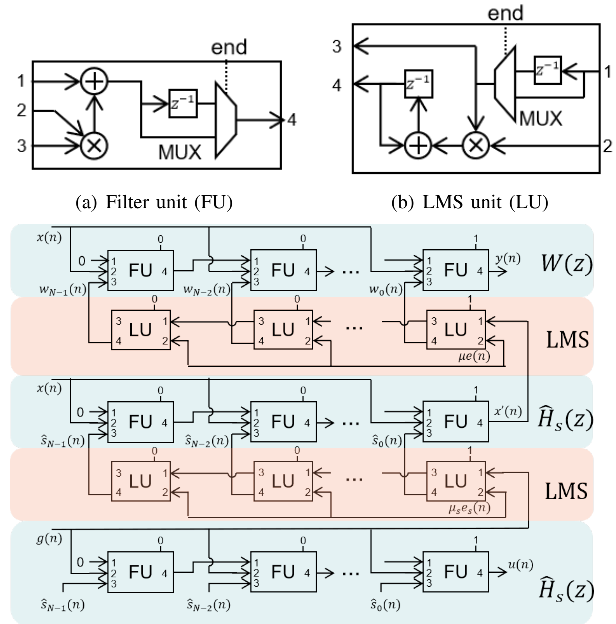

(a) Filter unit (FU) (b) LMS unit (LU)

(c) Overall structure

Fig. 5: Systolic structure of the online modeling algorithm with additional white noise.

III. SYSTEM VALIDATION

The primary and secondary paths used in the system validation are shown in Fig. 6. They are measured from an experimental setup of the FFANC system. The primary noise is a bandlimited white noise, whose bandwidth is from 300 Hz to 1200 Hz. The additional white noise for online secondary path modeling is a fullband Gaussian noise, with a mean of zero and a variance of σ^2.

Figure 7 shows the three convergence curves for comparison. They are resultant from the Eriksson and Allie's original algorithm, the proposed systolic structure and the true digital FFANC system that further integrates two PDM demodulators and one PDM modulator. The control filter (400 taps) and the secondary path model (200 taps) are both initialized with zero. The step sizes for updating the control filter and the secondary path model are set at $\mu_w = 0.008$ and $\mu_s = 0.016$, respectively. The standard deviation of the additional white noise increases from 0.005 to 0.02 to present four different scenarios. It is observed that when the additional white noise level is higher, the ANC system achieves its steady state earlier, since the secondary path modeling is completed faster, but the residual noise level is also higher.

Figure 8 shows another comparison of convergence curves when the standard deviation of the additional white noise is fixed at 0.01. The step sizes for updating the control filter and the secondary path model are set to different values to present four different scenarios. It is observed that when the step sizes are large, the systolic structure results in a slightly slower convergence as compared to Eriksson and Allie's original

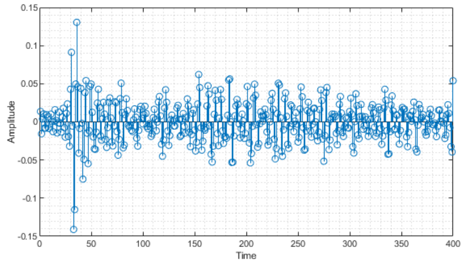

(a) Impulse response of the primary path (400 taps)

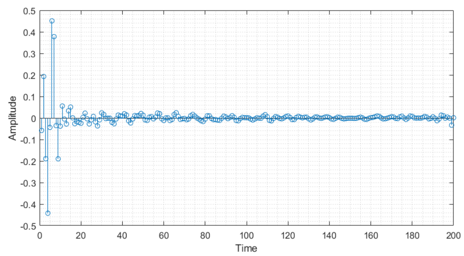

(b) Impulse response of the secondary path (200 taps)

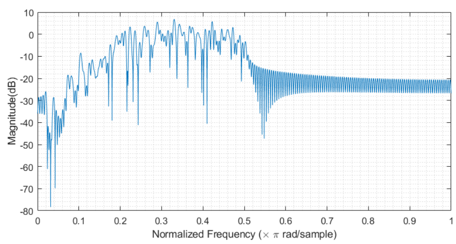

(c) Frequency response of the primary path

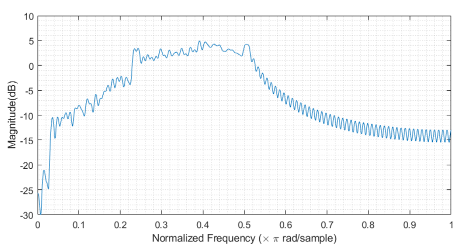

(d) Frequency response of the secondary path

Fig. 6: Primary and secondary paths used in the system validation.

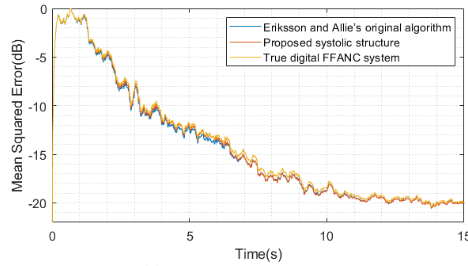

(a) μ_w = 0.008, μ_s = 0.016, σ = 0.005

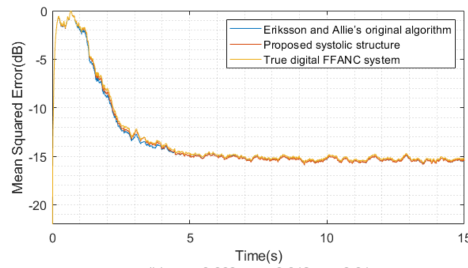

(b) μ_w = 0.008, μ_s = 0.016, σ = 0.01

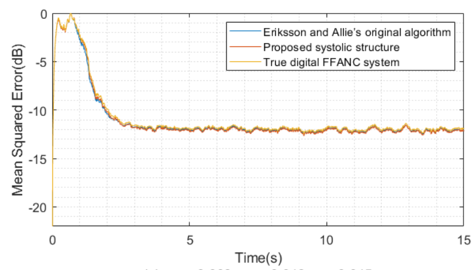

(c) μ_w = 0.008, μ_s = 0.016, σ = 0.015

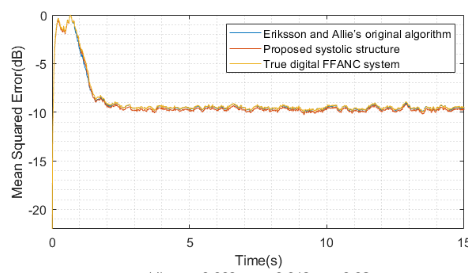

(d) μ_w = 0.008, μ_s = 0.016, σ = 0.02

Fig. 7: Convergence curves of Eriksson and Allie's original algorithm, the proposed systolic structure and the true digital FFANC system with $\mu_w = 0.008$ and $\mu_s = 0.016$, under different levels of additional white noise.

algorithm, while the PDM demodulator and modulator have yet to show notable effect on the algorithm performance.

IV. Conclusions

This paper develops a true digital FFANC system on an FPGA, with PDM microphones and loudspeakers connected directly to its I/O pins. This true digital FFANC system requires no AD and DA converters, but efforts have been put into the design of the PDM demodulator and the PDM modulator. The online modeling algorithm with additional white noise is implemented by a pipelined systolic structure. Simulation results have validated that the performance of the true digital ANC system is close to Eriksson and Allie's original algorithm most of the time when the step sizes are set small. This is an inherited characteristic of the systolic structure, which can be traced back to the delayed LMS algorithm.

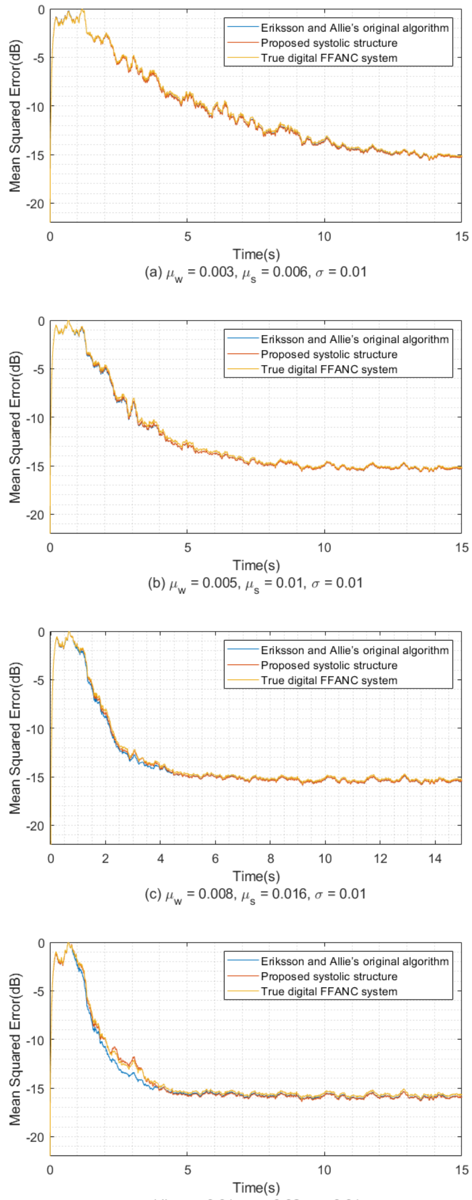

(a) $\mu_w = 0.003$, $\mu_s = 0.006$, $\sigma = 0.01$

(b) $\mu_w = 0.005$, $\mu_s = 0.01$, $\sigma = 0.01$

(c) $\mu_w = 0.008$, $\mu_s = 0.016$, $\sigma = 0.01$

(d) $\mu_w = 0.01$, $\mu_s = 0.02$, $\sigma = 0.01$

Fig. 8: Convergence curves of Eriksson and Allie's original algorithm, the proposed systolic structure and the true digital FFANC system with $\sigma = 0.01$, under different settings of μ_w and μ_s.

Acknowledgment

This manuscript is prepared based on the research work supported by the National Natural Science Foundation of China and the Civil Aviation Administration of China (Joint Grant No. U1933127).

References

[1] C. H. Hansen, *Understanding active noise cancellation*. Spon Press: London, 2001.

[2] S. J. Elliott, *Signal processing for active control*. Academic Press: London, 2000.

[3] Y. Kajikawa, W. S. Gan, and S. M. Kuo, "Recent advances on active noise control: Open issues and innovative applications," *APSIPA Transactions on Signal and Inforamtion Processing*, vol. 1, no. e3, pp. 1–21, 2012.

[4] S. J. Elliott, I. Stothers, and P. A. Nelson, "A multiple error LMS algorithm and its application to the active control of sound and vibration," *IEEE Transactions on Acoustics, Speech, and Signal Processing*, vol. 35, no. 10, pp. 1423-1434, 1987.

[5] C. Shi, R. Xie, N. Jiang, H. Li, and Y. Kajikawa, "Selective virtual sensing technique for multi-channel feedforward active noise control systems," *Proceedings of the 44th IEEE International Conference on Acoustics, Speech and Signal Processing*, Brighton, United Kingdom, 2019.

[6] C. Shi, Z. Jia, R. Xie, and H. Li, "An active noise control casing using the multi-channel feedforward control system and the relative path based virtual sensing method," *Mechnical Systems and Signal Processing*, vol. 144, 2020.

[7] H. A. Sanchez-Hevia, R. Gil-Pita, and M. Rosa-Zurera, "FPGA-based real-time acoustic camera using PDM MEMS microphones with a custom demouldation filter," *Proceedings of the 8th IEEE Sensor Array and Multichannel Signal Processing Workshop*, A Coruna, Spain, 2014.

[8] P. M. Aziz, H. V. Sorensen, and J. vn der Spiegel, "An overview of sigma-delta converters," *IEEE Signal Processing Magazine*, vol. 13, no. 1, pp. 61-84, 1996.

[9] L. K. Ting, R. Woods, and C. F. N. Cowan, "Virtex FPGA implementation of a pipelined adaptive LMS predictor for electronic support measures receivers," *IEEE Transactions on Very Large Scale Integration (VLSI) Systems*, vol. 13, no. 1, pp. 86-95, 2005.

[10] D. Shi, J. He, C. Shi, T. Murao, and W. S. Gan, "Multiple parallel branch with folding architecture for multichannel filtered-x least mean square algorithm," *Proceedings of the 42nd IEEE International Conference on Acoustics, Speech and Signal Processing*, New Orleans, United States, 2017.

[11] D. Shi, W. S. Gan, J. He, and B. Lam, "Practical implementation of multichannel filtered-x least mean square algorithm based on the multiple-parallel-branch with folding architecture for large-scale active noise control," *IEEE Transactions on Very Large Scale Integration (VLSI) Systems*, vol. 28, no. 4, 2020.

[12] Y. Gao, L. Jia, and H. Tenhunen, "A partial-polyphase VLSI architecture for very high speed CIC decimation filters," *Proceedings of the 12th Annual IEEE International ASIC/SOC Conference*, Washington, United States, 1999, pp. 391-395.

[13] A. Y. Kwentus, Z. Jiang, and A. N. Willson, "Application of filter sharpening to cascaded integrator-comb decimation filters," *IEEE Transactions on Signal Processing*, vol. 45, no. 2, pp. 457-467, 1997.

[14] R. Adams, P. Ferguson, A. Ganesan, S. Vincelette, A. Volpe, and R. Libert, "Theory and practical implementation of a fifth-order sigma-delta A/D converter," *Journal of the Audio Engineering Society*, vol. 39, pp. 515-528, 1991.

[15] S. Pavan, R. Schreier, and G. C. Temes, *Understanding delta-sigma data converters*. Wiley-IEEE Press: New Jersey, 2017.

[16] J. C. Burgess, "Active adaptive sound control in a duct: A computer simulation," *Journal of the Acoustical Society of America*, vol. 70, no. 3, pp. 715-726, 1981.

[17] C. Shi and Y. Kajikawa, "A partial-update minimax algorithm for practical implementation of multi-channel feedforward active noise control," *Proceedings of the 2018 International Workshop on Acoustic Signal Enhancement*, Tokyo, Japan, 2018.

[18] C. Shi, Z. Yuan, R. Xie, and H. Li, "Simultaneous variable perturbation method for the active noise control system with a wireless error microphone," *Proceedings of the 2020 Asia-Pacific Signal and Information Processing Association Annual Summit and Conference*, Auckland, New Zealand, 2020.

[19] L. J. Eriksson and M. C. Allie, "Use of random noise for on-line transducer modeling in an adaptive active attenuation system," *Journal of the Acoustical Society of America*, vol. 85, no. 2, pp. 797–802, 1989.

[20] D. Shi, C. Shi, and W. Gan, "A systolic FxLMS structure for implementation of feedforward active noise control on FPGA," *Proceedings of the 2016 Asia-Pacific Signal and Information Processing Association Annual Summit and Conference*, Jeju, Korea, 2016.